Biochemistry

 Volume 32, Number 50 December 21, 1993

Accelerated Publications

Structure of Toxic Shock Syndrome Toxin 1[†,‡]

G. Sridhar Prasad,[⊥] Cathleen A. Earhart,[⊥] Debra L. Murray,[§] Richard P. Novick,[∥] Patrick M. Schlievert,[§] and Douglas H. Ohlendorf*[,⊥]

Departments of Biochemistry and Microbiology, University of Minnesota Medical School, Minneapolis, Minnesota 55455, and Public Health Research Institute of the City of New York, New York, New York 10016

Received October 8, 1993; Revised Manuscript Received October 22, 1993[●]

ABSTRACT: The three-dimensional structure of toxic shock syndrome toxin 1 (TSST-1) from *Staphylococcus aureus* has been determined and refined to an *R* value of 0.226 for data between 8- and 2.5-Å resolution. Overall, the structure of TSST-1 is similar to that of another superantigen, staphylococcal enterotoxin B (SEB). The key differences between these molecules are in the amino termini and in the degree to which a long central helix is covered by surface loops. The region around the carboxyl end of this central helix is proposed to govern the superantigenic properties of TSST-1. An adjacent region along this helix is proposed to be critical in the ability of TSST-1 to induce toxic shock syndrome.

Toxic shock syndrome toxin-1 (TSST-1),[1] the major cause of TSS, belongs to a large family of exotoxins made by *Staphylococcus aureus* and streptococci, particularly group A. These protein toxins, including TSST-1, staphylococcal enterotoxins serotypes A to G but excluding F, group A streptococcal pyrogenic exotoxins serotypes A to C (scarlet fever toxins), and a recently described group B streptococcal pyrogenic exotoxin, share numerous immunobiological properties. These include the induction of fever, the enhancement of host susceptibility to lethal endotoxin shock, the induction of capillary leakage, and the induction of T lymphocyte proliferation dependent upon interaction with certain T cell receptor β chain variable regions (White et al., 1989; Marrack & Kappler, 1990; Bohach et al., 1990). For example, in patients with TSS as many as 60% of their peripheral blood lymphocytes during the acute illness may display T cell receptors containing the Vβ2 amino acid sequence resulting from stimulation by TSST-1 of all such T cells (Choi et al., 1990). This T cell proliferation has led to the toxins being referred to as superantigens (Marrack & Kappler, 1990). The superantigenicity depends first on the interaction of toxin with MHC class II molecules outside of the antigen-binding site and subsequently on the interaction of the toxin–MHC class II complex with the T cell receptor. These toxins are proposed to have separate domains for binding to MHC class II molecules and the T cell receptor (Dellabona et al., 1990; Karp et al., 1990; Marrack & Kappler, 1990).

Within the last year the three-dimensional structure of staphylococcal enterotoxin B has been solved (Swaminathan et al., 1992). SEB folds into a kidney-shaped molecule with two domains each composed largely of β strands. The central region connecting these domains has three α helices. SEB shares highly significant primary sequence similarity with many other members of the larger toxin family, most notably

† This work has been partially supported by grants from the National Institutes of Health (GM-46436 to D.H.O. and AI-22159 to R.P.N. and P.M.S.) and from the Minnesota Supercomputer Institute to D.H.O. G.S.P. was supported by grants from Kimberly-Clark Corp., Neenah, WI, from Personal Products Co., New Brunswick, NJ, and from Tambrands, Palmer, MA.

‡ The coordinates have been deposited in the Brookhaven Protein Data Bank under the file name 1TSS.

* To whom correspondence should be addressed.

⊥ Department of Biochemistry, University of Minnesota Medical School.

§ Department of Microbiology, University of Minnesota Medical School.

∥ Public Health Research Institute of the City of New York.

● Abstract published in *Advance ACS Abstracts*, December 1, 1993.

[1] Abbreviations: TSST-1, toxic shock syndrome toxin-1; TSS, toxic shock syndrome; SEB, staphylococcal enterotoxin B; MHC, major histocompatibility complex.

0006-2960/93/0432-13761$04.00/0

Table I: Structure Determination and Refinement Statistics[a]

compound	resolution (Å)	completeness	R_{sym} [b]	R_{iso} [c]	R_{Cullis} [d]	figure of merit	phasing power[e]	number of sites
native	2.05	0.98	0.067					
7.5 mM ammonium diuranate	4.0	0.88	0.134	0.223	0.55	0.45	1.83	3
5 mM ammonium diuranate	4.0	0.97	0.119	0.201	0.64	0.41	1.63	3
2 mM potassium uranyl fluoride	3.6	0.69	0.168	0.190	0.68	0.37	0.92	5
2 mM potassium hexacyanoplatinate	3.4	0.90	0.128	0.150	0.71	0.35	0.76	2
4 mM potassium osmium hexachloride	4.0	0.96	0.086	0.190	0.66	0.41	0.94	6
3 mM rhenium chloride	3.0	0.80	0.108	0.240	0.67	0.43	0.97	6

[a] R value (R value = $\sum_{hkl}|F_o - F_c|/\sum_{hkl}F_o$) = 0.226 for 28 624 reflections between 8 and 2.5 Å with $I > 2\sigma$. R free (R free = R value for a set of reflections not used in refinement) = 0.319. RMS deviation in bond lengths = 0.016 Å. RMS deviation in bond angles = 2.2°. [b] $R_{sym} = \sum_{hkl}\sum_i|I_i(hkl) - \langle I(hkl)\rangle|/\sum_{hkl}\sum_i I_i(hkl)$. [c] $R_{iso} = \sum_{hkl}|F_{PH} - F_P|/\sum_{hkl}F_P$. [d] $R_{Cullis} = \sum_{hkl}|F_{PH} \pm F_P| - F_H^{calc}|/\sum_{hkl}|F_{PH} + F_P|$ for centric reflections. [e] Phasing power = $\langle F_H\rangle/E$ where E is the RMS lack of closure.

with SEC and streptococcal pyrogenic exotoxin A. Interestingly, TSST-1 shares little (20–30%) primary sequence with SEB or other members of the family (Betley et al., 1992), yet it can be hypothesized that since TSST-1 shares biological activities with other members of the family, it likely shares at least some structural features. A determination of the structure of TSST-1 was undertaken as a step in the investigation of the differences and similarities of this family of toxins.

MATERIALS AND METHODS

TSST-1 was purified and crystallized in several forms as previously described (Earhart et al., 1993). The $C222_1$ crystals of TSST-1 were chosen for analysis due to the high order to which diffraction was observed, i.e., 2.05 Å. The unit cell lengths are a = 108.7 Å, b = 177.5 Å, and c = 97.6 Å. An initial analysis of the diffraction using the rotation function indicated the presence of a local three-fold axis parallel to the crystallographic **c** axis with local two-fold axes every 60° in the **ab** plane (Earhart et al., 1993). From these data it was concluded that the asymmetric unit contains three molecules of TSST-1.

Multiple isomorphous replacement was used to solve the structure of TSST-1 (see Table I). Native and derivative data were collected using a Siemens area detector and monochromated Cu Kα radiation. The data frames were processed using the XENGEN suite of programs (Howard et al., 1987). Heavy atom phase refinement was done initially using the programs HEAVY (Terwilliger & Eisenberg, 1983). Initial electron density maps to 4-Å resolution were calculated using the program SQUASH (Zhang & Main, 1990) to impose solvent flattening. The program MLPHARE (Leslie, 1988) was used to refine heavy atom phases against the phases produced by SQUASH.

A visual examination of heavy atom difference Fourier map for the ammonium diuranate derivative indicated monomers of TSST-1 were related to one another by a pseudo-6_122 symmetry. Knowledge of the local symmetry aided in the interpretation of the heavy atom derivatives and provided initial estimates of the transformations relating the three molecules of TSST-1 in the asymmetric unit. The refined transformations were obtained by using the RAVE package of programs (G. J. Kleywegt and T. A. Jones, personal communication) to maximize the correlation among spherical regions of the electron density map. A modified version of SQUASH (D. Schuller, personal communication) was used for density averaging, solvent flattening, and phase extension to 3.1-Å resolution.

The resulting electron density map was exceptionally clear (see Figure 1). The program MAID (Levitt & Banaszak, 1993) was used to build the initial model of TSST-1. The model was subjected to molecular dynamics refinement (Brünger et al., 1987) using the data between 8- and 3.2-Å resolution. After a round of temperature factor refinement, the R value was 0.216 for data with $I > 2\sigma$. At this point the occupancies of residues Thr 75, Ser 76, and Glu 77 were set to zero due to lack of well-defined electron density, and data to 2.5 Å were included. After a second round of molecular dynamics refinement and temperature factor refinement the model presented here was obtained. The R value is 0.226 to 2.5-Å resolution with good geometry (See Table I).

During the refinement, the three molecules of TSST-1 were not constrained by the local symmetry. The RMS agreement between molecules is 0.5 Å using Cα's and 1.1 Å using all atoms. Because of this similarity, no distinction between molecules will be made in the subsequent discussion.

RESULTS AND DISCUSSION

The ribbon drawing of the elements of secondary structure of TSST-1 is presented in Figure 2. The view presented in this figure will be considered the standard orientation with designations such as front or back referring to this orientation. TSST-1 is a kidney-shaped molecule approximately 55 Å × 40 Å × 35 Å. Domain A (on the left in Figure 2) is composed of residues 1–15 and 79–194. The principal feature of this domain is a 17-residue α helix (helix B, see Figure 3) on a five-strand mixed β sheet. Strands 10, 11, and 13 are adjacent and antiparallel as are strands 7 and 8. However, the adjacent strands 7 and 10 are parallel. At the top of the sheet and over the carboxyl end of helix B is the 12-residue helix A. Using the conventions of Richardson et al. (1976), the topology of the sheet is $+1,-3x,-1,+2x$ with both crossovers being right-handed. The smaller domain B (on the right in Figure 2) is a five-stranded mixed β barrel formed by residues 18–89. All pairs of adjacent strands in the barrel are antiparallel with the exception of strands 3 and 5. The topology of the barrel is $-1,-1,-2,+1$. The fold is also present in staphylococcal nuclease (Hynes & Fox, 1991). Between these proteins 80 Cα pairs can be superimposed with an RMS difference of 1.74 Å.

The surface of TSST-1 has two pronounced grooves in the middle of the molecule. The largest groove is on the back of TSST-1 with its walls rising from helix B. The walls of the groove are formed by helix A with its subsequent loop before strand 1 and by strand 9 with its preceding loop . The other groove is much smaller and on the front of TSST-1. It is bounded by the same amino-terminal segment just described, by domain B, and by helix D and the loop preceding it. Helix B is also at the bottom of this groove.

There are a large number of charged amino acids spread over the surface of TSST-1. This distribution is rather uniform but with two notable exceptions both in domain B. One is the

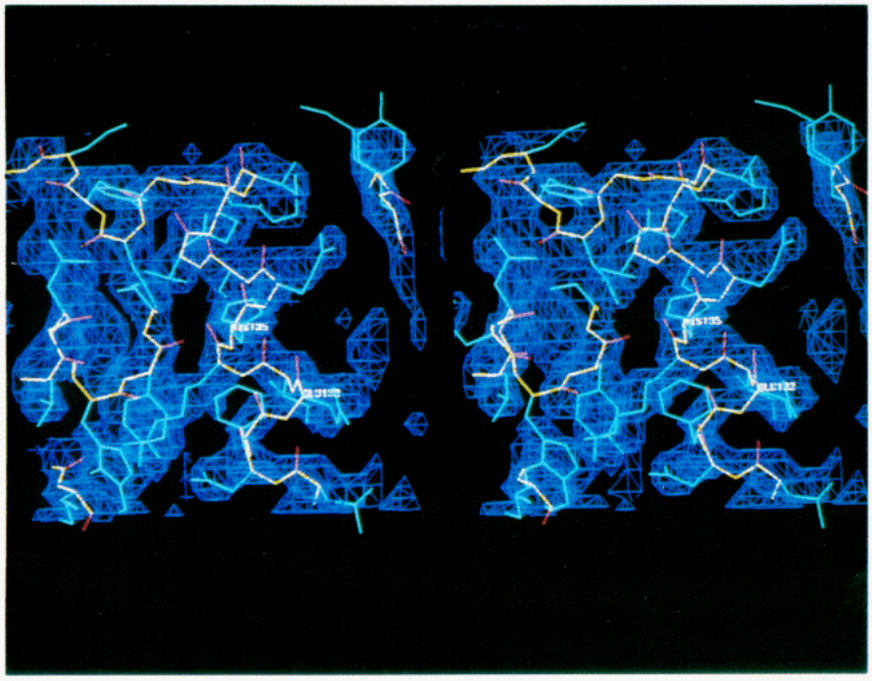

FIGURE 1: Initial electron density for TSST-1 calculated using multiple isomorphous replacement and averaging. The region display is the view into the groove on the back of the molecule onto helix B. Residues 135 and 132 are labeled. The structure presented is the partially refined model.

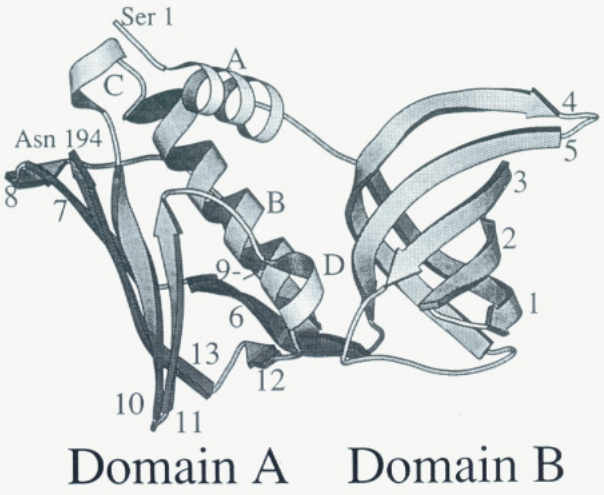

FIGURE 2: Ribbon drawing of showing the secondary structural elements of TSST-1 in standard orientation. Helices are labeled A–D and are represented as coils. β strands are labeled 1–13 and are shown as arrows.

top surface of the barrel formed by strand 4 which contains five basic residues (Lys 67, Arg 68, Lys 70, Lys 71, and His 74). The second is an area of approximately 300 Å^2 on the front of domain B which contains no charged residues. This region encompasses the carboxyl ends of strands 1, 3, and 5, the amino ends of strand 2, and helix D. The residues involved are Ser 29, Leu 30, Ser 32, Leu 44, Ile 46, Pro 48, Pro 50, Thr 69, Asn 175, and Tyr 174.

Although generally similar, there are several differences between the structures of TSST-1 and SEB (Swaminathan et al., 1992). Figure 3 shows an alignment of the amino acid sequences of TSST-1 and SEB using common secondary structural elements. This alignment has a number of differences from that proposed by Betley and Mekalanos (1988) and reflects the low sequence homology between the two molecules. One difference between SEB and TSST-1 is at the amino terminus. TSST-1 has only two residues before helix A. In SEB, there are 20 residues before the helix α2.

Another difference between these two toxins is in the loops connecting the β strands in domain B. Specifically, in TSST-1 the loop connecting strands 1 and 2 is short, and the ends of duplex wrap around the barrel. In SEB, the loop and some adjacent residues appear to be peeled back from the barrel. The loop connecting strands 3 and 4 in TSST-1 has an open, extended conformation. In SEB this loop is more compact and is folded to form a nine-residue helix (α3). In TSST-1 strands 4 and 5 form hydrogen bonds to nearly the end of the loop which projects away from the toxin. In SEB this loop is larger and has an irregular conformation. In TSST-1 there is no clear electron density for the final three residues in the loop. In SEB there is no electron density for residues 99–105 (Swaminathan et al., 1992). In SEB, this loop contains a number of basic amino acids (Lys 98, Lys 99, His 105, Lys 109, Arg 110, and Lys 111) which make the top of domain B strongly basic as it is in TSST-1.

An important difference between TSST-1 and SEB is the extent to which helix B (α4) is covered on the front and back of each toxin. In TSST-1 the back of domain A contains a rather large loop including strand 9 that is roughly parallel to the axis of helix B. This loop covers nearly all of the back surface of the helix. In the front of TSST-1 is a loop formed by residues 169–184 containing helix D and strand 12. This loop also is roughly parallel to the axis of helix B and covers much of the front surface of the helix. However, since both loops do not extend above or to the right of helix B as depicted in Figure 2, residues of that helix which face domain B are accessible from the top of TSST-1. In SEB, residues 141–151 form strand β7 which hydrogen bonds with strand β6. This has two effects. One is to lower the segment corresponding to residues 109–124 exposing nearly all of the back surface of the central helix. The second effect is to produce a more highly twisted β sheet in domain A in SEB. In the front of SEB, residues 201–229 form a large flap that lies over the right half of domain A. This flap allows only a portion of Asp 161 and Arg 165 on the front surface of the central helix to be exposed (Swaminathan et al., 1992). Thus, while the central

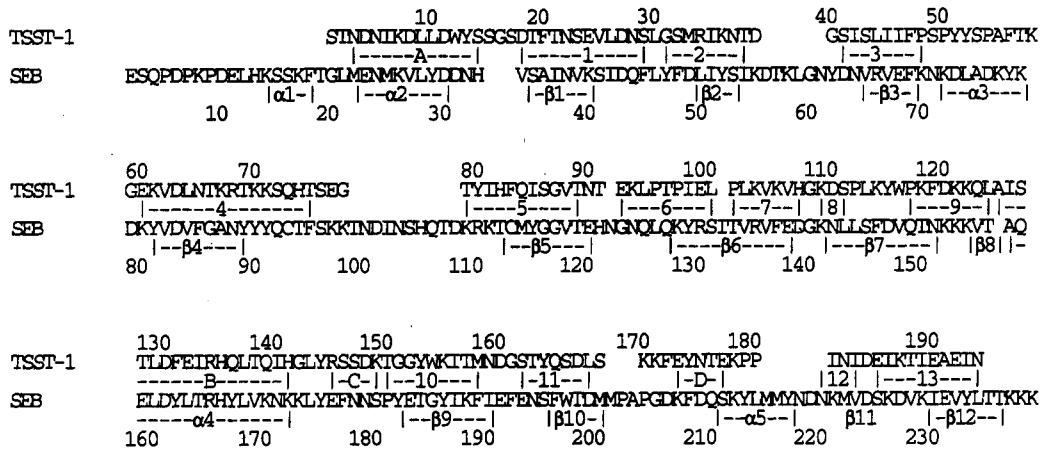

FIGURE 3: Alignment of amino sequences of TSST-1 and of SEB keyed on common structural features. The secondary structural elements are labeled under each sequence. Residue number for each protein are provided. The labeling and assignment of the secondary structure of SEB is that reported by Swaminathan et al. (1992).

helix is significantly more exposed on the back side of SEB than is the case in TSST-1, the front side of SEB is completely covered by this large flap.

Two distinct activities of TSST-1 are important to consider: (1) interaction with MHC class II and the T cell receptor resulting in superantigenicity and (2) induction of toxic shock syndrome and associate lethality. Biochemical studies of TSST-1 have suggested portions of the molecule that are functionally significant. Early studies by Blomster-Hautamaa et al. (1986) found that a polypeptide composed of residues 34–158 which is produced by treatment with CNBr binds monoclonal antibodies that block the mitogenic and immunosuppressive properties of TSST-1. Subsequent experiments by Edwin and Kass (1989) showed that two carboxyl-terminal polypeptides produced by papain treatment have superantigenic activity and can bind neutralizing antibodies. These polypeptides result from cleavage of the peptide bonds between Gly 87 and Val 88 or between Tyr 52 and Ser 53. Taken together these data suggest that the region containing residues 88–158 is likely to be important for the function of TSST-1. From the structure, this region can be seen to extend from the interface of domains A and B, through the loop covering the back surface helix B, helices B and C, and strand 10. In addition, the results of Edwin and Kass (1989) suggest that in solution there is at least transient separation of the two domains. This conclusion can be made because the papain cleavage site between Gly 87 and Val 88 is not accessible in the structure present in the crystal.

The analysis of a number of mutants of TSST-1 has provided more detailed information regarding key features of the toxin. These results are summarized in Table II. This work has focused on two properties of TSST-1, i.e., its toxicity to the host and its ability to stimulate T cell proliferation. Several techniques have been used to assay the results of the mutations. One is the effectiveness of the mutant in binding monoclonal antibodies that neutralize the lethality and/or the superantigenicity of the toxin. A second technique is to measure directly the lethal levels of TSST-1 using either continuous injection of purified toxin over an extended period using a miniosmotic pump, a single injection of TSST-1 followed by an injection of endotoxin, or placing TSST-1 producing organisms in a porous subcutaneous chamber. This latter technique is no longer in wide use because one cannot control for the amount of toxin produced. Thus, results using this assay can be highly variable. A third technique for characterizing the mutants is through a direct assay of mitogenicity.

Table II: Properties of TSST-1 and Mutants

mutation	binding of neutralizing[a] antibodies	lethality: mini-osmotic pump	lethality: endotoxin enhancement	lethality: subcutaneous chambers	superantigenicity
TSST-1	++	+	+	+	++++
Y80A, H82A	+	nd[b]	nd	0[c]	++++
Y115A	–	nd	nd	0	++
H135A	+	nd	nd	–	–
H141A	+	nd	nd	0	++
H141A, Y144A	–	nd	nd	0	–
TSST-O[d]	+	–	–	nd	+
E132K, I140T	+	–	–	nd	–
I140T	+	+	+	nd	++

[a] In the first group of mutants monoclonal antibody 8-5-7 was used by Bonventre and colleagues (Blanco et al., 1990; Bonventre et al., 1993), which neutralizes both superantigenicity and lethality. In the second group of mutants monoclonal antibodies B-14, which neutralizes superantigenicity but not lethality, and 12–13, which neutralizes lethality but not superantigenicity, were used (Murray et al., 1993). [b] Not determined. [c] Some toxicity, but not enough animals were tested to evaluate its significance. [d] Isolated from Ovine mastitis = [T19A, A55T, T57S, Y80W, E132K, I140T].

Since superantigens such as TSST-1 and SEB must interact with both a class II MHC and the T cell receptor, destruction of either binding site will block this activity.

A number of mutants have been made which show no change in biological activity tested. These are [Y51A,Y52A], H74A, and Y153A (Blanco et al., 1990; Bonventre et al., 1993). Tyr 51 and Tyr 52 are located in the interface between domains A and B at the bottom of the molecule in the loop connecting strands 3 and 4 (see Figure 2). Tyr 51 is exposed and Tyr 52 is buried in the interface. The next mutation (H74A) is in strand 4 at the top of the barrel of domain B. Its side chain is highly exposed and projects upward. [Y80A, H82A] shows no significant biological effects. Tyr 80 and His 82 are in strand 5 on the inner surface of the barrel and are close to His 74. These results suggest that the top surface of domain B is not likely to be involved with either lethality or mitogenicity. However, the comparable region in SEB does seem to be important in producing emetic activity. In SEB as in the other enterotoxins this segment forms an open disulfide loop. Since TSST-1 has no cysteinyl residues, it cannot form the disulfide loop. This difference has been suggested as a partial explanation of the lack of emetic activity in TSST-1 (Spero & Morlock, 1978). The other mutant, Y153A, is found on the outer surface of strand 10.

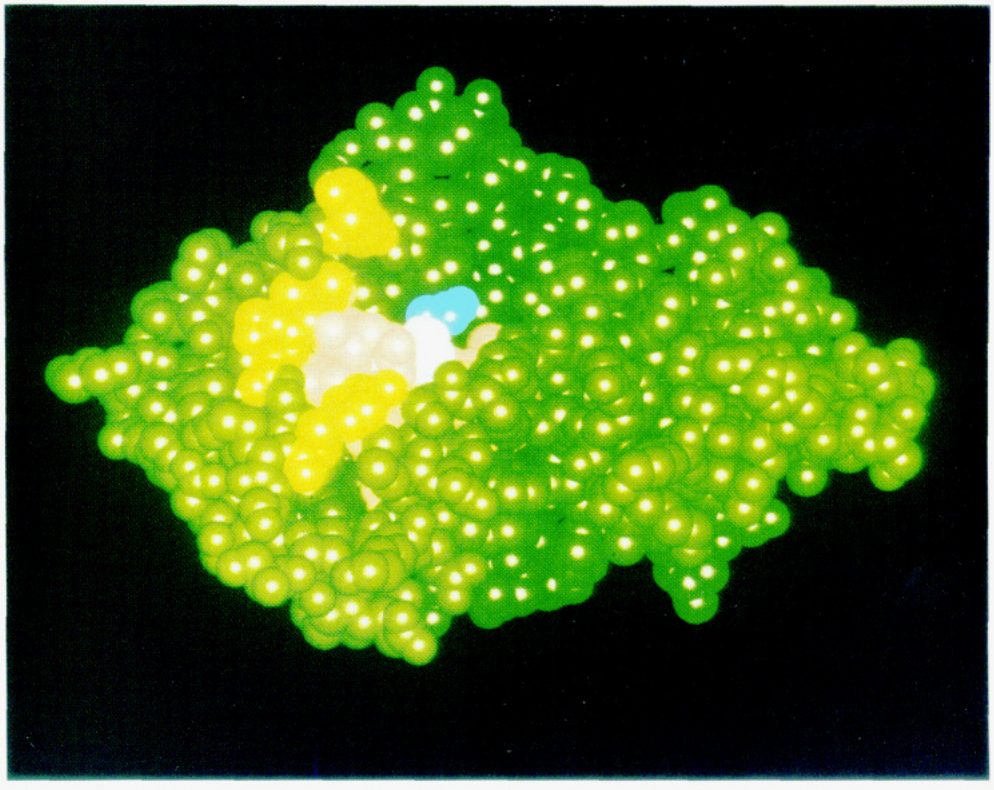

FIGURE 4: Space-filling drawing of the top surface of TSST-1. Residues in helix B are colored pink, residue 132 is colored blue, residue 135 is colored white, and residues 115, 140, 141, and 144 are colored yellow.

Several mutations influence mitogenicity. Y115A and [H141A, Y144A] both reduce superantigenicity and do not bind to superantigen-neutralizing antibodies. These residues are on the top of domain A (see Figure 4). His 141 is at the carboxyl end of helix B and has only one face of the side chain exposed. The 50% reduction in superantigenicity caused by this mutation may result from a small conformation shift. Tyr 115 is at the top of the loop on the back of TSST-1 that covers the back of helix B. The side chain projects away from the molecule and is maximally exposed. Tyr 144 is at the carboxyl end of helix B and has a large solvent-accessible area. The mutant H135A is not superantigenic but does bind an antibody that blocks superantigenicity in wild-type TSST-1. His 135 is in helix B, two turns below Tyr 144. Two other mutations that reduce superantigenicity are I140T and [E132K, I140T]. Ile 140 is also found at the carboxyl end of helix B while Glu 132 is two turns of the helix away. These results suggest that the carboxyl end of helix B and residues at the top of domain A form a surface that is critical for superantigenicity. The fact that Y115A exhibits altered binding to a neutralizing antibody suggests that the antibody-recognition surface is also on the top of domain A.

A smaller number of mutations have been shown to influence the lethality of TSST-1. TSST-O is different from TSST-1 in seven positions. Six of the seven changes are conservative changes that are spread over the surface of the molecule. The other change (E132K) shifts the pI of the molecule from 7.2 to 8.5 (Ho et al., 1989). Long-term, continuous injection of TSST-O does not lead to toxic shock syndrome in the rabbit model nor does it potentiate endotoxin shock (Lee et al., 1992). It is also only weakly mitogenic. The [E132K, I140T] mutant which is not lethal shows that it is these residues that are primarily responsible for these altered properties. Since the single mutant I140T shows no reduction in lethality, the E132K mutation must be responsible for this effect. Consequently, we propose that the amino-terminal half of helix B forms part of the surface that governs this property. The fact that I140T and [E132K, I140T] show reduced binding to a monoclonal antibody that blocks lethality suggests that the recognition surface for this antibody extends across the top of domain A in such a way that access to residue 132 is altered.

A similar analysis has been made by Swaminathan et al. (1992) of SEB mutants. They propose that the T cell receptor binding site is at the top of SEB at the interface of the two domains and across the top of domain B covering the conserved Asn 23 in SEB. This residue in TSST-1 is Asn 5 and is at the amino-terminal end of helix A. As for the MHC binding site, they suggest that residues in the center of both the front and back of SEB may be involved. If this is the case, then the significant structural differences exhibited on these surfaces combined with the ability of both toxins to bind to the same MHC class II molecules are consistent with the presence of distinct binding sites for the two toxins as reported by Scholl et al. (1989).

In conclusion, despite weak primary homology, the structure of TSST-1 is similar to that of SEB. Examination of the structures of these molecules in light of the results of mutational analysis suggest that the superantigenicity of these molecules involves the region surrounding the carboxyl end of the central helix. For SEB and TSST-1 the exposures of the central helix are distinct with varying amounts covered by surface loops. In addition, since the amino terminus of each toxin is in this region, the differing number of residues before helix A (α2) may also be significant in controlling this interaction. It appears likely that it is these differences which govern the phenomenon of superantigenicity. The data from mutant toxins suggest that the lethality and superantigenicity of TSST-1 are separate phenomena (Murray et al., 1993). This analysis suggests that the amino-terminal half of the central helix is important in controlling the lethality of TSST-1.

Understanding the structural foundations of the biological effects of these molecules will allow the design of a new generation of antitumor agents (Hedlund et al., 1993) in which superantigenicity is retained but lethality has been eliminated.

ACKNOWLEDGMENT

We thank Debi Leverich for technical assistance and Dr. R. Radhakrishnan, Dr. David Schuller, and Dr. David Levitt for helpful observations and computational assistance.

REFERENCES

Betley, M. J., & Mekalanos, J. J. (1988) *J. Bacteriol. 170*, 34–41.

Betley, M. J., Borst, D. W., & Regassa, L. B. (1992) *Chem. Immunol. 55*, 1–35.

Blanco, L., Choi, E. M., Connolly, K., Thompson, M. R., & Bonventre, P. F. (1990) *Infect. Immun. 58*, 3020–3028.

Blomster-Hautamaa, D. A., Novick R. N., & Schlievert, P. M. (1986) *J. Immunol. 137*, 3572–3576.

Bohach, G. A., Fast, D. J., Nelson, R. D., & Schlievert, P. M. (1990) *Crit. Rev. Microbiol. 17*, 251–272.

Bonventre, P. F., Heeg, H., Cullen, C., & Lian, C. J. (1993) *Infect. Immun. 61*, 793–799.

Brünger, A. T., Kuriyan, J., & Karplus, M. (1987) *Science 235*, 458–460.

Choi, Y., Lafferty, J. A., Clements, J. R., Todd, J. K., Gelfand, E. W., Kappler, J., & Marrack, P. (1990) *J. Exp. Med. 172*, 981–984.

Dellabona, P., Peccoud, J., Kappler, J., Marrack, P., Benoist, C., & Mathis, D. (1990) *Cell 62*, 1115–1121.

Earhart, C. A., Prasad, G. S., Murray, D. L., Novick, R. P., Schlievert, P. M., & Ohlendorf, D. H. (1993) *Proteins: Struct., Funct., Genet. 17*, 329–334.

Hedlund, G., Dohlsten, M., Petersson, C., & Kalland, T. (1993) *Cancer Immunol. Immunother. 36*, 89–93.

Ho, G., Campbell, W. H., & Carlson, E. (1989) *J. Clin. Microbiol. 27*, 210–212.

Howard, A. J., Gilliland, G. L., Finzel, B. C., Poulos, T. L., Ohlendorf, D. H., & Salemme, F. R. (1987) *J. Appl. Crystallogr. 20*, 383–387.

Hynes, T., & Fox, R. O. (1991) *Proteins 10*, 92–105.

Karp, D. R., Teletski, C. L., Scholl, P., Geha, R., & Long, E. O. (1990) *Nature 346*, 474–476.

Lee, P. K., Kreiswirth, B. N., Deringer, J. R., Projan, S. J., Eisner, W., Smith, B. L., Carlson, E., Novick, R. N., & Schlievert, P. M. (1992) *J. Infect. Dis. 165*, 1056–1063.

Leslie, A. G. W. (1988) *Improving Protein Phases*. Proceedings of the Daresbury Study Weekend, pp 25–31, SERC Daresbury Laboratory, Warrington, England.

Levitt, D. G., & Banaszak, L. J. (1993) *J. Appl. Crystallogr. 26* 736–745.

Marrack, P., & Kappler, J. W. (1990) *Science 248*, 705–711.

Murray, D. L., Prasad, G. S., Garhart, C. A., Leonard, B. A. B., Kreiswirth, B. N., Novick, R. P., Ohlendort, D. H., & Schlievert, P. M. (1993) *J. Immunol.* (in press).

Richardson J. S., Richardson, D. C., Thomas, K. A., Silverton, E. W., & Davies, D. R. (1976) *J. Mol. Biol. 102*, 221–235.

Spero, L., & Morlock, B. A. (1978) *J. Biol. Chem. 253*, 8787–8791.

Swaminathan, S., Furey, W., Pletcher, J., & Sax, M. (1992) *Nature 359*, 801–806.

Terwilliger, T. C., & Eisenberg, D. (1983) *Acta Crystallogr. A39*, 813–817.

White, J., Herman, A., Pullen, A. M., Kubo, R., Kappler, J. W., & Marrack, P. (1989) *Cell 56*, 27–35.

Zhang, K. Y. J., & Main, P. (1990) *Acta Crystallogr. A46*, 377–381.